

EVENT PILEUP IN CHARGE-COUPLED DEVICES

JOHN E. DAVIS

Center for Space Research Chandra X-Ray Center, 70 Vassar Street, NE080-6019 Massachusetts Institute of Technology, Cambridge, MA 02139;
davis@space.mit.edu

Received 2001 January 16; accepted 2001 July 25

ABSTRACT

The problem of event pileup in single-photon-counting CCD cameras (e.g., in the X-ray regime) is discussed, and a solution to the problem is proposed. The resulting pileup equation includes the effects of grade migration and presents itself as a nonlinear modification to the standard integral equation used by forward-folding spectral-fitting programs. The effectiveness of the model is demonstrated by its application to the moderately piled zeroth-order data obtained by the *Chandra X-Ray Observatory* for the quasar S5 0836 + 7104.

Subject headings: instrumentation: detectors — methods: analytical — methods: data analysis — X-rays: general

1. INTRODUCTION

Pileup in a charge-coupled device (CCD) is a phenomena associated with the finite temporal and spatial resolution of the CCD and is defined as the coincidence of two or more photons per CCD time-resolution element, or frame-time, within an event-detection cell. The detector will be unable to temporally resolve two or more photons that interact in a detection cell if they occur during an integration period, resulting in a pulse height that is roughly the sum of the pulse heights of the individual photon events. Hence, in the presence of pileup, the event-detection rate will be lower, and the observed spectrum will be distorted toward higher energies (see Fig. 1).

The standard procedure (Gorenstein, Gursky, & Garmire 1968) for the spectral analysis of point sources in X-ray astronomy relies on the use of the integral equation (Davis 2001)

$$C(h) = (N\tau) \int dE R(h, E)A(E)s(E), \quad (1)$$

which relates the number of observed counts $C(h)$ in the pulse-height channel h during an effective exposure time $(N\tau)$ to the incident source spectrum $s(E)$. The function $A(E)$ represents the energy-dependent effective area of the system and $R(h, E)$ represents the probability for the redistribution of energy E into a pulse-height channel h by the detector. However, equation (1) is a *linear* integral equation, whereas pileup is inherently a *nonlinear* process. Hence, the treatment of pileup lies outside the domain of applicability of this equation. The inadequacy of equation (1) when applied to a spectrum affected by pileup is illustrated in Figure 2. This paper proposes an alternative integral equation that can be used in place of equation (1) when the effects of pileup are important.

Any treatment of pileup has to take into account the effects of “grade migration.” When a photon lands in a CCD pixel, it creates a charge cloud that can be split across neighboring pixels. This splitting pattern can be classified according to its shape and labeled by a number called a “grade” (see Fig. 3). The reason for doing this is that true X-ray events are much more likely to produce some grades than others. Hence, filtering of the grade of an event tends to increase the signal-to-noise ratio of the CCD by the rejection of unwanted events, such as those generated by cosmic-ray interactions, which are known to produce a different

grade distribution. The problem with pileup is that two or more piled photons may also produce events with an undesirable grade. This phenomena is known as grade migration and leads to further suppression of the count rate because grade filtering throws such events away. Any prescription for dealing with pileup must take this important effect into account.

Most discussions of pileup have centered around the question of how one can estimate the degree of pileup for a specific observation, largely for the purpose of proposal planning (see, e.g., the 1999 ACIS Cal Report).¹ An exception worth noting is the work of Ballet (1999), who considered the effects of grade migration and concluded that single-pixel events are likely to be unaffected by pileup. Hence, he argued that one could perform spectral analysis on single-pixel events using the standard technique based on equation (1). The main problems with his approach are that there are likely to be few single-pixel events, and that the calibration information appropriate to such non-standard event filtering may be lacking.

The next section considers the response of the CCD to n piled photons and addresses the problem of grade migration. The formulation of an integral equation describing the effects of pileup in a single detection cell is presented in § 3. The effectiveness of the resulting pileup model is demonstrated in § 4 by its application to a moderately piled data set obtained by the *Chandra X-Ray Observatory* for the quasar S5 0836 + 7104. The paper concludes with a discussion of the limits of the pileup model and a brief summary of the results of the paper. An appendix describes a practical realization of the model as implemented in the ISIS spectral-modeling program (Houck & DeNicola 1999),² which was used for the analysis of the S5 0836 + 7104 data.

2. THE CCD RESPONSE FOR PILED PHOTONS

A precise formulation of pileup would involve a detailed microscopic theory solidly grounded in solid-state physics. The approach taken here is much less ambitious and largely phenomenological. It is based on the assertion that the

¹ A postscript version of the Science Instrument Calibration Report for the AXAF CCD Imaging Spectrometer, Version 2.20, 1999, is available at http://asc.harvard.edu/cal/Links/Acis/acis/Cal_prods/cal_report.ps.

² Houck & DeNicola 2000 is available at Web site <http://space.mit.edu/ASC/ISIS>.

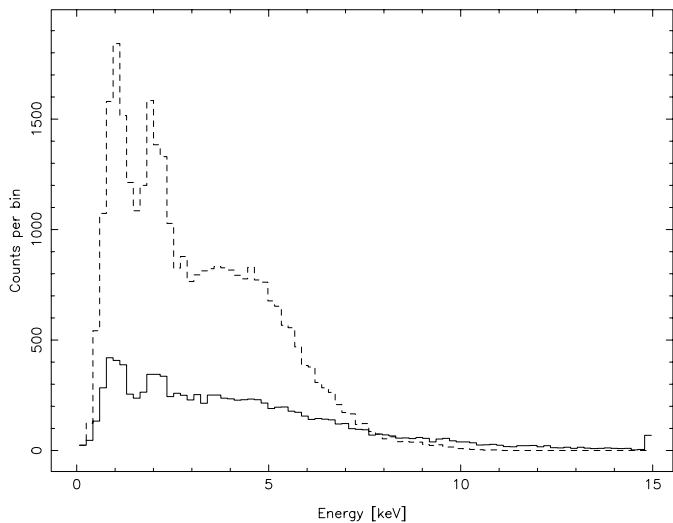


FIG. 1.—Effects of pileup. The upper (*dashed*) curve shows the expected PHA spectrum from S5 0836+7104 in the absence of pileup, as predicted by a MARX simulation. The lower (*solid*) curve shows the actual observed PHA spectrum. Note that the observed count rate is about 3 times lower than expected and that the observed PHA spectrum extends to much higher energies. Both of these effects are a direct result of pileup.

resulting charge cloud of two or more piled photons can be regarded as the linear superposition of the individual charge clouds that would have been generated by each of the participating photons in the absence of pileup. The independence of the charge clouds stems from the fact that the drift time for the charge clouds is on the order of microseconds, which is much smaller than the integration time between readouts.

To express this idea in mathematical terms, let $D_i(h, E)$ be the probability that a photon of energy E incident upon the CCD will give rise to an event with pulse height h and grade i . Here an event is graded as either “good” or “bad,” with $i = 0$ representing a good grade and $i = 1$ representing a

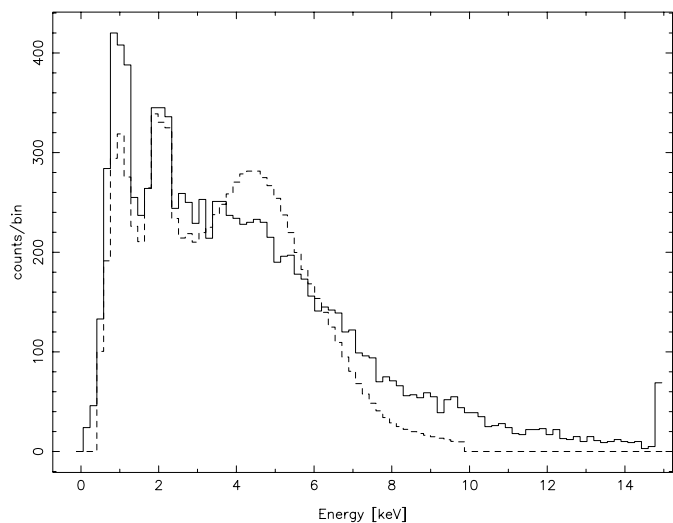


FIG. 2.—Failure of the standard technique based on the use of eq. (1), when applied to the piled CCD data of S5 0836+7104 (*solid curve*). The spectral fit, shown here as the *dashed curve*, was performed using eq. (1) and assuming an absorbed power law for the spectrum. The best-fit parameters of this fit are given in Table 1.

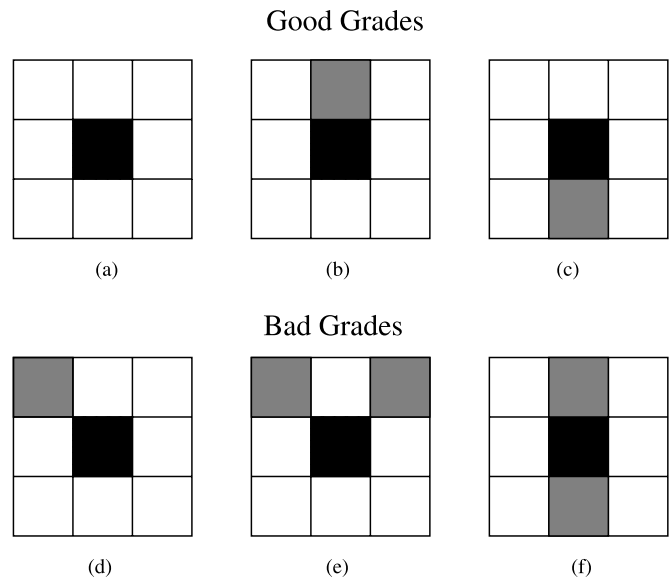


FIG. 3.—Event grades and grade migration. The top portion of the figure shows three examples of charge-cloud splitting patterns that correspond to events with good grades. The bottom portion of the figure shows three examples of patterns representing bad grades, which are unlikely to be produced as a result of a single photon interaction. In each of these cases, the dark pixel at the center of the 3×3 pixel event-detection cell contains more charge than any of its eight neighbors (i.e., it is a local maximum). Each of the lighter shaded pixels contains charge that is above some threshold, whereas the unshaded pixels are below the threshold. Note that the bad-grade pattern illustrated in (*f*) can be obtained by a superposition of the two good-grade patterns, (*b*) and (*c*). This effect whereby two (or more) photons pile up to produce an event with a bad grade is known as “grade migration.”

bad grade (see Fig. 3). Further refinement of the grades is unnecessary in what follows. For the moment, the response of the CCD is assumed to be spatially invariant. The function $D_i(h, E)$ can be factored as

$$D_i(h, E) = R_i(h, E)g_i(E)Q_{\text{bare}}(E), \quad (2)$$

where $R_i(h, E)$ represents the redistribution by the detector of energy E to pulse height h , and is assumed to be normalized according to

$$1 = \sum_h R_i(h, E). \quad (3)$$

Similarly, the function $g_i(E)$, representing the probability that the event will be assigned the grade i , satisfies

$$1 = \sum_i g_i(E). \quad (4)$$

The quantity $Q_{\text{bare}}(E)$ is called the “bare” quantum efficiency (QE) because its value does not depend on the act of grade selection. Customarily, when one speaks of the QE, one almost always is referring to the *measured* QE for good events, denoted here simply as $Q(E)$. It is related to the bare QE via

$$Q(E) = g_0(E)Q_{\text{bare}}(E). \quad (5)$$

Similarly, $R_0(h, E)$ corresponds to the measured redistribution function for good events and can be written simply as $R(h, E)$.

With the above definitions in place, consider the case of two piled photons, one with energy E_1 and the other with energy E_2 . The probability $D_k(h, E_1, E_2)$ that these photons will produce a grade k event with pulse height h is assumed

to be given by the superposition of individual events, i.e.,

$$\begin{aligned}
 D_k(h, E_1, E_2) &= \sum_{ij} \sum_{h' < h} G_k^{ij}(E_1, E_2) D_i(h', E_1) \\
 &\quad \times D_j(h - h', E_2) \\
 &= \sum_{ij} \sum_{h' < h} G_k^{ij}(E_1, E_2) R_i(h', E_1) \\
 &\quad \times R_j(h - h', E_2) \\
 &\quad \times g_i(E_1) g_j(E_2) Q_{\text{bare}}(E_1) Q_{\text{bare}}(E_2). \quad (6)
 \end{aligned}$$

The function $G_k^{ij}(E_1, E_2)$ represents the probability that a grade i producing charge cloud generated by a photon with energy E_1 and a grade j producing cloud generated by a photon with energy E_2 will combine to form a grade k event. It is assumed to obey the symmetry relation

$$G_k^{ij}(E_1, E_2) = G_k^{ji}(E_2, E_1), \quad (7)$$

and satisfy

$$1 = \sum_k G_k^{ij}(E_1, E_2). \quad (8)$$

It is reasonable to assume that $G_0^{ij}(E_1, E_2)$ will be much smaller than $G_0^{00}(E_1, E_2)$ if either i or j corresponds to unwanted grade, since a bad grade producing charge cloud is unlikely to combine with another to produce a good event. For this reason, the term involving $G_0^{00}(E_1, E_2)$ is expected to dominate the sum, thereby permitting the approximation

$$\begin{aligned}
 D_0(h, E_1, E_2) &\approx G_0^{00}(E_1, E_2) Q(E_1) Q(E_2) \\
 &\quad \times \sum_{h' < h} R_0(h', E_1) R_0(h - h', E_2). \quad (9)
 \end{aligned}$$

Moreover, as stated in the introduction, the purpose of grade selection is to maximize the signal-to-noise ratio by discarding events that are unlikely to be produced by X-rays. Hence, one would expect $g_0(E)$ to be much larger than $g_1(E)$ for sources that are not too hard, and as long as one is interested only in good events, then the dominant term in equation (6) for $k = 0$ is once again the $i = j = 0$ term.

For a detector whose response $R(h, E)$ consists of a single Gaussian with a width proportional to $E^{1/2}$, centered on a pulse height that scales linearly with E , it is easy to show that

$$R(h, E_1 + E_2) = \sum_{h' < h} R(h', E_1) R(h - h', E_2). \quad (10)$$

In addition to the main peak, a realistic CCD response function will also contain fluorescence and escape peaks. Hence, strictly speaking, the previous equation is not generally true.

The fluorescence yield in silicon is about 4% for the silicon K-shell. That is, about 4% of the time, a photon with energy above about 1.86 keV will give rise to a fluorescence photon by first knocking out a K-shell electron. The actual percentage is smaller than this because a certain fraction of the time, the fluorescence photon will be reabsorbed by the CCD to pile with the original photon. Hence, at most, fluorescence is a few percent effect.

Assuming that one can safely neglect fluorescence events, the two-photon function $D_0(h, E_1, E_2)$ is assumed to be given by

$$D_0(h, E_1, E_2) \approx G_2(E_1, E_2) R(h, E_1 + E_2) Q(E_1) Q(E_2), \quad (11)$$

where for notational simplicity, $G_0^{00}(E_1, E_2)$ has been written as $G_2(E_1, E_2)$. Similar reasoning can be used to obtain

$$\begin{aligned}
 D_0(h, E_1, E_2, \dots, E_n) &\approx G_n(E_1, E_2, \dots, E_n) \\
 &\quad \times R(h, E_1 + E_2 + \dots + E_n) \\
 &\quad \times Q(E_1) Q(E_2) \dots Q(E_n) \quad (12)
 \end{aligned}$$

for the n -photon response function. This equation is also valid for $n = 1$, provided that one defines $G_1(E_1) = 1$.

The function $G_n(E_1, E_2, \dots, E_n)$ represents the effect of grade migration for n piled photons. It gives the probability for the event produced by n piled photons to have a good grade. In general, this probability depends on the energies of the individual piling photons. More is said about this in the next section.

Before leaving this section, it is perhaps worthwhile to discuss the dependence of the response functions on the locations of the charge clouds in the detection cell. First of all, consider the dependence of the single-photon response function $R(h, E)$ on the position of the charge cloud. Clearly, the actual splitting pattern depends on the location of the charge cloud. For instance, a charge cloud located near the edge of a pixel is much more likely to produce a pulse height in the nearest neighboring pixel than a charge cloud located at the center of a pixel. Naively, it would appear that $R(h, E)$ is sensitive to the position of the charge cloud. However, as long as the resulting splitting pattern is likely to be part of the good grade set, $R(h, E)$ itself may not be too sensitive to the charge cloud's location within the detection cell.

Unfortunately, this is not true for the grade migration functions $G_n(E_1, \dots, E_n)$, since they determine the probability for n charge clouds to produce a pattern representing a good grade. In other words, the grade migration functions may depend on the locations of the charge clouds and should be written as $G_n(E_1, \dots, E_n, \sigma_1, \dots, \sigma_n)$ to reflect the dependence on the positions σ_i of the charge clouds within a detection cell. The photons are distributed over an event-detection cell according to a probability distribution determined by the point-spread function (PSF) and the spatial distribution of the source. Hence, only grade migration functions that have been averaged over this probability distribution will be used in practice. Such functions will be denoted by $\langle G_n(E_1, \dots, E_n) \rangle$.

3. A PILEUP MODEL

The goal of this section is to formulate an integral equation connecting an incident source distribution $s(E, \hat{p})$ to the expected number of counts $C(h)$ in a pulse-height channel h . Here, $s(E, \hat{p})$ is defined such that $s(E, \hat{p}) dE d\hat{p}$ denotes the number of photons per unit area per unit time incident upon the telescope with directions in the cone of directions between \hat{p} and $\hat{p} + d\hat{p}$, and with energies between E and $E + dE$.

Let $\xi(E, \sigma) \Delta\sigma$ represent the number of photons $\text{keV}^{-1} \text{s}^{-1}$ that produce charge clouds in a region of size $\Delta\sigma$ located at the position σ on the detector. It is related to the incident source distribution $s(E, \hat{p})$ by (Davis 2001)

$$\xi(E, \sigma) = \int d\hat{p} Q_{\text{bare}}(E, \sigma) \mathcal{F}(E, \sigma, \hat{p}) M(E, \hat{p}) s(E, \hat{p}). \quad (13)$$

Here, $M(E, \hat{p})$ represents the effective area of the mirror as a function of photon energy and off-axis angle. The PSF of the mirror is represented by $\mathcal{F}(E, \sigma, \hat{p})$, which gives the probability that a photon with energy E and direction \hat{p} will be reflected by the mirror to the position σ on the detector.

Denoting the region occupied by a detection cell by ω , it follows that the number of charge clouds produced per second in the region ω by photons with energies between E and $E + \Delta E$ is given by

$$\begin{aligned} \xi_\omega(E)\Delta E &= \Delta E \int_\omega d\sigma \xi(E, \sigma) \\ &= \Delta E \int d\hat{p} A_{\omega, \text{bare}}(E, \hat{p}) s(E, \hat{p}). \end{aligned} \quad (14)$$

The quantity $A_{\omega, \text{bare}}(E, \hat{p})$, defined by

$$A_{\omega, \text{bare}}(E, \hat{p}) = \int_\omega d\sigma Q_{\text{bare}}(E, \sigma) \mathcal{F}(E, \sigma, \hat{p}) M(E, \hat{p}), \quad (15)$$

represents the effective area for a photon with energy E incident upon the telescope with a direction \hat{p} to give rise to a pulse height producing a charge cloud in the region ω . It is related to the effective area $A_\omega(E, \hat{p})$ for producing charge clouds with good grades by the expression

$$A_\omega(E, \hat{p}) = g_0(E) A_{\omega, \text{bare}}(E, \hat{p}). \quad (16)$$

Assuming that the photon arrival times are Poisson-distributed, it follows from simple Poisson statistics that the probability of having n_1 photons with energies between E_1 and $E_1 + \Delta E$, n_2 photons with energies between E_2 and $E_2 + \Delta E$, and so on, producing charge clouds in the event-detection cell ω within a frame-time τ , is given by

$$\prod_{i=1}^{\infty} \frac{[\tau \xi_\omega(E_i) \Delta E]^{n_i}}{n_i!} e^{-\tau \xi_\omega(E_i) \Delta E}. \quad (17)$$

Using the results of the previous section, it is easy to see that the probability for this configuration of photons to produce an event with a good grade and pulse height h during the time interval τ is given by

$$\begin{aligned} e^{-\tau \sum_i \xi_\omega(E_i) \Delta E} R(h, \sum_i n_i E_i) \langle G_{n_1 n_2 \dots}(E_1, E_2, \dots) \rangle \\ \times \prod_i \frac{[\tau g_0(E_i) \xi_\omega(E_i) \Delta E]^{n_i}}{n_i!}, \end{aligned} \quad (18)$$

where for notational simplicity, $\langle G_{n_1 n_2 \dots}(E_1, E_2, \dots) \rangle$ denotes the spatially averaged grade migration function appropriate for this particular combination of photons, i.e., represents $\langle G_{n_1 + n_2 + \dots}(E_1, \dots, E_2, \dots) \rangle$ with each E_i occurring n_i times.

Summing this expression over all possible photon number configurations and multiplying by the total number of frames³ N yields

$$\begin{aligned} C_\omega(h) &= N e^{-\tau \sum_i \xi_\omega(E_i) \Delta E} \\ &\times \sum_{\{n_1 n_2 \dots\}} \left\{ R(h, \sum_i n_i E_i) \langle G_{n_1 n_2 \dots}(E_1, E_2, \dots) \rangle \right. \\ &\times \left. \prod_i \frac{[\tau g_0(E_i) \xi_\omega(E_i) \Delta E]^{n_i}}{n_i!} \right\}, \end{aligned} \quad (19)$$

which is the total number of counts with pulse height h expected after N frames in the detection cell ω . One can

show that this sum can be written as

$$C_\omega(h) = \sum_{p=1}^{\infty} C_{\omega, p}(h), \quad (20)$$

where

$$\begin{aligned} C_{\omega, p}(h) &= N e^{-\tau \sum_i \xi_\omega(E_i) \Delta E} \\ &\times \frac{\tau^p}{p!} \sum_{i_1 \dots i_p} [\langle G_p(E_{i_1}, \dots, E_{i_p}) \rangle R(h, E_{i_1} + \dots E_{i_p}) \\ &\times g_0(E_{i_1}) \xi_\omega(E_{i_1}) \Delta E \dots g_0(E_{i_p}) \xi_\omega(E_{i_p}) \Delta E] \end{aligned} \quad (21)$$

is the contribution to the expected number of counts with pulse height h from p piled photons. Substituting equations (14) and (16) into the previous equation and taking the continuum limit $\Delta E \rightarrow 0$ yields

$$\begin{aligned} C_\omega(h) &= N e^{-\tau \int dE \int d\hat{p} A_{\omega, \text{bare}}(E, \hat{p}) s(E, \hat{p})} \\ &\times \sum_{p=1}^{\infty} \left[\frac{\tau^p}{p!} \int_0^\infty dE_1 \dots \int_0^\infty dE_p \langle G_p(E_1, \dots, E_p) \rangle \right. \\ &\times \left. R\left(h, \sum_{i=1}^p E_i\right) \prod_{i=1}^p \int d\hat{p} A_\omega(E_i, \hat{p}) s(E_i, \hat{p}) \right]. \end{aligned} \quad (22)$$

The no-pileup case is obtained by letting τ go to zero and N go to infinity such that the product $N\tau$ remains constant. This prescription yields the familiar equation (Davis 2001)

$$C_\omega(h) = (N\tau) \int dE R(h, E) \int d\hat{p} A_\omega(E, \hat{p}) s(E, \hat{p}), \quad (23)$$

which is used for the spectral analysis of nonpiled X-ray sources.

When the effects of pileup are important, the preceding equation is inadequate, forcing one to consider equation (22) instead. At first sight, this does not look practical because not only does it depend on the (possibly unknown) grade migration functions $\langle G_p(E_1, \dots, E_p) \rangle$, but the numerical computation of the effect of p piled photons appears to scale exponentially with p . However, as shown below, the grade migration functions can be dealt with in a practical manner, and the computation time can be made to scale linearly with p .

Although each of the grade migration functions $\langle G_p(E_1, \dots, E_p) \rangle$ can be a very complicated function of the photon energies, their probabilistic interpretations require that the range of the functions lie somewhere between zero and one. Because of this constraint, a multidimensional integral of the form

$$\int_0^\infty dE_1 \dots \int_0^\infty dE_p \langle G_p(E_1, \dots, E_p) \rangle H_\omega(E_1, \dots, E_p; h), \quad (24)$$

where $H_\omega(E_1, \dots, E_p; h)$ is an arbitrary nonnegative function, is equal⁴ to

$$\bar{G}_{p, \omega}(h) \int_0^\infty dE_1 \dots \int_0^\infty dE_p H_\omega(E_1, \dots, E_p; h), \quad (25)$$

⁴ This is essentially a variation of the so-called mean value theorem of integral calculus.

³ Dropped frames are not included in the value of N .

for some function $\bar{G}_{p,\omega}(h)$ satisfying $0 \leq \bar{G}_{p,\omega}(h) \leq 1$. Of course, the actual functional form of $\bar{G}_{p,\omega}(h)$ depends on the function $H_\omega(E_1, \dots, E_p; h)$. The basic idea is to use this fact to replace the functions $\langle G_p(E_1, \dots, E_p) \rangle$ in equation (22) by a set of functions $\{\bar{G}_{p,\omega}(h)\}$, to be determined during the spectral-fitting process, as described below. Similarly, in accordance with equation (16), $A_{\omega, \text{bare}}(E, \hat{p})$ is replaced by $A_\omega(E, \hat{p})/\bar{g}_{0,\omega}$, with $\bar{g}_{0,\omega}$ to be determined. After making these changes, introduce a delta function into equation (22) to rewrite it as

$$C_\omega(h) = Ne^{-\tau/\bar{g}_{0,\omega}} \int dE f(E) \times \int dE R(h, E) \sum_{p=1}^{\infty} \frac{\tau^p \bar{G}_{p,\omega}(h)}{p!} \times \left[\int_0^\infty dE_1 \dots \int_0^\infty dE_p \delta\left(E - \sum_{i=1}^p E_i\right) \prod_{i=1}^p f(E_i) \right], \quad (26)$$

where for clarity,

$$f(E) = \int d\hat{p} A_\omega(E, \hat{p}) s(E, \hat{p}). \quad (27)$$

Now consider the $p = 2$ term in the square brackets, written here as

$$\int_0^\infty dE' \int_0^\infty dE'' f(E') f(E'') \delta(E - E' - E''). \quad (28)$$

The integration over E'' can be readily performed to yield

$$\int_0^\infty dE' f(E - E') f(E'). \quad (29)$$

By defining $s(E - E', \hat{p})$, and hence $f(E - E')$, to be zero for $E < E'$, the upper limit on the integral can be reduced to E , i.e.,

$$\int_0^E dE' f(E - E') f(E'), \quad (30)$$

which is just the convolution of $f(E)$ with itself. That is, the integral in the $p = 2$ term can be written as $f(E) * f(E)$, where the $*$ operator specifies the ‘‘convolution product.’’ Similarly, as the reader can easily show,

$$[f(E)]^{*p} = \int_0^\infty dE_1 \dots \int_0^\infty dE_p \delta\left(E - \sum_{i=1}^p E_i\right) \prod_{i=1}^p f(E_i), \quad (31)$$

where $[f(E)]^{*p}$ signifies the p th convolution product of $f(E)$ with itself. Thus, equation (26) can be written in the form

$$C_\omega(h) = Ne^{-\tau/\bar{g}_{0,\omega}} \int dE \int d\hat{p} A_\omega(E, \hat{p}) s(E, \hat{p}) \times \int dE R(h, E) \sum_{p=1}^{\infty} \bar{G}_{p,\omega}(h) \frac{[\tau \int d\hat{p} A_\omega(E, \hat{p}) s(E, \hat{p})]^{*p}}{p!}. \quad (32)$$

Note that the evaluation of the p th term in the series involves p convolution products. In other words, the actual computation time for the contribution due to p piling photons scales linearly with p .

Equation (32) is the main result of this work. It is a non-linear integral equation connecting an incident source distribution $s(E, \hat{p})$ to the expected number of counts $C_\omega(h)$ with pulse height h in a detection cell ω . It depends on the functions $\{\bar{G}_2(h, \omega), \bar{G}_3(h, \omega), \dots\}$, representing the effects of

grade migration, and $\bar{g}_{0,\omega}$, which gives the probability for a single photon event having a good grade.

Before applying equation (32), it is necessary to specify the grade migration functions $\bar{G}_{p,\omega}(h)$. Recall that $\bar{G}_{p,\omega}(h)$ represents the probability for the charge clouds of p photons to merge to produce an event with a good grade in the region ω . One would expect this probability to be largely determined by the relative spacing of the charge clouds. For example, the merger of two charge clouds from different parts of an event-detection cell is likely to yield a different event grade than two charge clouds produced at the same place. Hence, as long as there is a significant probability for the two charge clouds to be produced at different places within the event-detection cell, $\bar{G}_{p,\omega}(h)$ is likely to be relatively insensitive to h . This is almost certainly true for any detector whose pixel size is of the order of the PSF size or smaller, as is the case for *Chandra*/ACIS. Hence, for all practical purposes, $\bar{G}_{p,\omega}(h)$ can be assumed to be a slowly varying function of h .

Finally, in order to make use of equation (32), it is necessary to reduce the infinite set of parameters $\{\bar{G}_{p,\omega}(h)\}$ to a more manageable set. Perhaps the simplest physically plausible parameterization in terms of a single, region-dependent parameter α_ω is

$$\bar{G}_{p,\omega}(h) = \alpha_\omega^{p-1}, \quad (33)$$

where $0 \leq \alpha_\omega \leq 1$. This particular choice of parameterization is consistent with the idea that the more photons that pile together, the more likely it is to produce an event with an unwanted grade. Since $\bar{G}_{p,\omega}(h)$ is expected to depend weakly on h , α_ω will also depend weakly on h . In this paper, α_ω is taken to be independent of h .

4. APPLICATION TO S5 0836 + 7104

S5 0836 + 7104, the brightest known quasar with a redshift greater than 2, was observed by the *Chandra X-Ray Observatory* on 1999 October 17. The observation was made using the High Energy Transmission Grating (HETG) in conjunction with the Advanced CCD Imaging Spectrometer (ACIS) for an effective exposure time of about 60 ks (Fang et al. 2001). This particular observation was chosen as a test case for the testing of the pileup model because the incident spectrum $s(E)$ could be easily obtained from the analysis of the first-order grating spectrum.

The CCD zeroth-order data were extracted and analyzed using a combination of standard CIAO tools and custom software. In particular, equation (32) was implemented as described in the Appendix for the ISIS spectral-modeling program, which was subsequently used for fitting the zeroth-order data. Data were extracted in sky coordinates from a circle with a 2'' radius centered on the location of the point source. The observation was made essentially on-axis, and from the work of Jerius et al. (2000), the PSF fraction within this region was estimated to be about 95%.

For simplicity, as described in the Appendix, it was assumed that the data could be modeled by considering two regions: a central region containing a single 3×3 pixel detection cell, where pileup was assumed to occur, and an outer region assumed to be free of pileup. From Figure 4, it can be seen that the smallest circle containing the 3×3 pixel pileup region has a radius of $1.5 \times \sqrt{2}$ ACIS pixels, or about 1''. The PSF fraction contained within such a circle was estimated to be about 90% (Jerius et al. 2000), or about

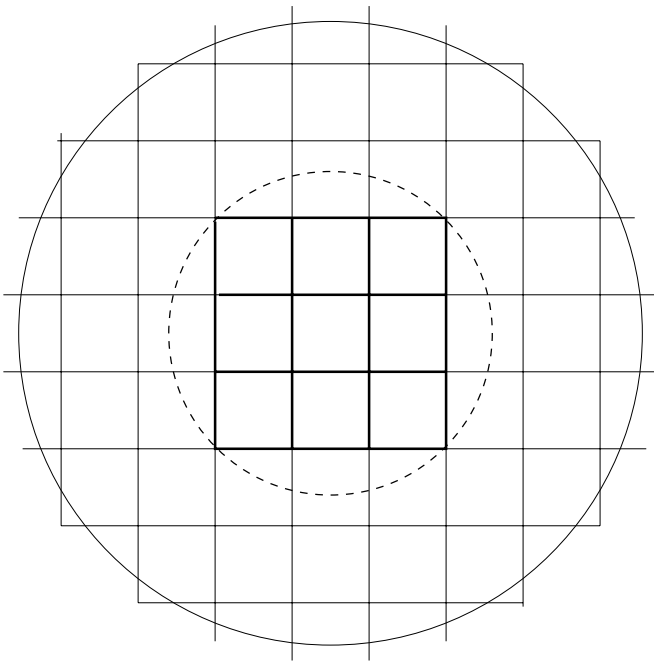


FIG. 4.—Extraction region and the 3×3 event-detection cell where pileup was expected to occur. As explained in the text, 95% of the flux falling into the extraction region was concentrated inside the inner circle enclosing the central 3×3 event-detection cell.

95% of the total PSF fraction contained within the full $2''$ extraction region.

An absorbed power law of the form

$$s(E) = \mathcal{N} e^{-N_{\text{H}} \sigma(E)} E^{-\Gamma} \quad (34)$$

was used to model the spectrum, and the spectral parameters (column density N_{H} , normalization \mathcal{N} , and spectral index Γ) were obtained via a χ^2 minimization procedure. In addition to varying the three model parameters, the grade-migration factor α was also allowed to vary. The quantity \bar{g}_0 , representing the branching ratio into good grades, was fixed at 1.0 in accordance with known calibration information (ACIS Cal Report 1999).¹ Problems associated with calibration uncertainties below 0.5 and above 10 keV prevented the modeling of the pulse-height analyzer (PHA) spectrum in those regions.

The pileup model fitted to the piled zeroth-order spectrum is shown in Figure 5, and the best-fit spectral parameters are given in Table 1. The table also illustrates the accuracy of the pileup model by a comparison of the spec-

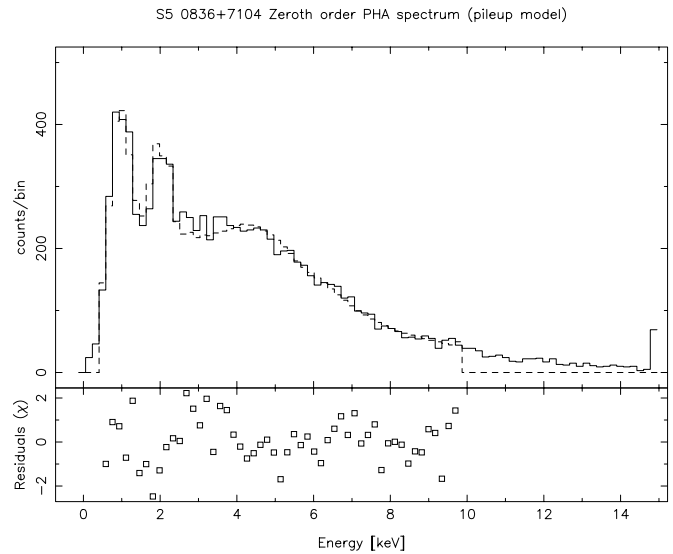


FIG. 5.—Best fit (*dashed curve*) to the zeroth-order CCD data (*solid curve*) using the pileup model of eq. (32). Data points below 0.5 keV were excluded from the fit because of calibration uncertainties in that energy region. Similarly, points above 10 keV were excluded because of the lack of calibration information in the low effective area region beyond 10 keV. The best-fit parameters are given in Table 1.

tral parameters deduced by it from the piled zeroth-order CCD data to those obtained by Fang et al. (2001) through direct modeling of the unpiled first-order HETG dispersed data.

5. DISCUSSION

As a result of pileup, the *observed* count rate goes to zero for large source fluxes; hence, any pileup model is useful only up to some maximum flux. Beyond that limit, the number of detected counts will be too small to be statistically relevant. This should not be seen as a weakness or failure of the pileup model, since the model is consistent with this behavior (see Fig. 6).

What is the maximum source flux to which the pileup model can be usefully applied? Unfortunately, this question has no unique answer. The useful range depends on many factors, including the shape of the PSF, the CCD frame time, and the nature of the source itself. For these reasons, it is strongly recommended that, when planning an observation of a bright source, one use realistic simulations to characterize the expected degree of pileup. Such simulated data sets can then be analyzed with the pileup model to determine whether or not one can recover the incident spec-

TABLE 1
SUMMARY OF SPECTRAL FITS

Analysis Method	N_{H} (10^{20} cm^{-2})	Spectral Index (Γ)	\mathcal{N}^a	α^b	$\tilde{\chi}^2/\text{dof}^c$
HETG ^d	7.0 ± 1.2^e	1.388 ± 0.012	$3.96^{+0.04}_{-0.07}$	N/A	1.072/605
Pileup model	5.5 ± 2.5	1.37 ± 0.08	4.21 ± 0.84	0.50 ± 0.02	1.068/50
Standard model ^f	0.001	0.76	0.57	N/A	12.81/51

^a Flux at 1 keV in units of $10^{-3} \text{ photons cm}^{-2} \text{ s}^{-1} \text{ keV}^{-1}$.

^b Based on the parametrization of eq. (33).

^c Reduced χ^2 .

^d Taken from Fang et al. 2001.

^e Confidence limits are quoted at the 90% level.

^f Based on eq. (1).

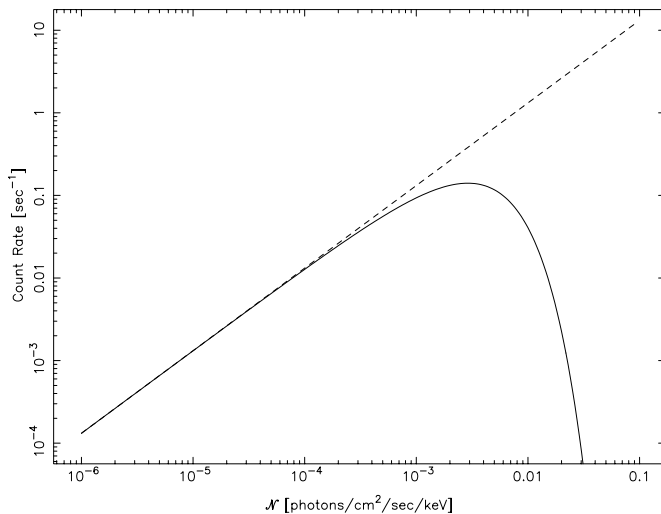


FIG. 6.—Effect of the flux normalization on the count rate. The dashed curve shows the count rate as predicted by the linear model of eq. (1). The solid curve shows the count rate as given by the pileup model for the observational parameters used for the S5 0836 + 7104 observation.

trum in a way that is statistically meaningful. By simulating the observation with various frame times and off-axis angles, one should be able to choose observation parameters that minimize the degree of pileup in a way that is consistent with the scientific goals of the observation.⁵

One technique for getting an estimate of the range of useful source fluxes is to use the pileup model itself as implemented in the ISIS spectral-modeling program. Figure 6 shows a plot of the expected count rate as a function of the flux normalization parameter \mathcal{N} for the absorbed power-law spectrum of equation (34). As the figure clearly shows, for small fluxes, the count rate increases linearly in accordance with the standard model of equation (1). However, at a flux normalization of about 10^{-4} photons $\text{cm}^{-2} \text{s}^{-1} \text{keV}^{-1}$, the nonlinear effects of pileup start to become important. After the count rate peaks at a flux of about 2.5×10^{-3} photons $\text{cm}^{-2} \text{s}^{-1} \text{keV}^{-1}$, it rapidly decreases and becomes effectively zero at 3×10^{-2} photons $\text{cm}^{-2} \text{s}^{-1} \text{keV}^{-1}$. Hence, this figure shows that the pileup model should be useful for fluxes that are 2 orders of magnitude larger than the flux at which the linear model starts to break down.

In the analysis of the *Chandra* observation of S5 0836 + 7104 described in § 4, pileup was assumed to occur in

⁵ An intriguing alternative made possible by an accurate pileup model is to choose observation parameters that *maximize* the detected count rate instead of those that minimize the degree of pileup.

a single detection cell. The validity of this assumption hinges on the size of the *Chandra* PSF, where for an on-axis point source, 90% of the flux is contained in a single 3×3 ACIS pixel region. In contrast, *XMM-Newton* has a much larger PSF and may require the use of multiple detection cells. For example, for the EPIC MOS detector, a 3×3 pixel region contains roughly 15% of the encircled energy (Aschenbach et al. 2000) for an on-axis point source. Moreover, the neighboring eight 3×3 detection cells share about 35% of the flux, giving an average PSF fraction of about 5% per cell. Hence, if the central detection cell experiences pileup, it is quite possible that the surrounding eight detection cells will also experience some degree of pileup. In any case, equation (32) should be directly applicable to *XMM-Newton* data, provided that one takes into account the PSF fraction enclosed by each detection cell.

6. CONCLUSION

The main result of this work was the formulation of an integral equation connecting an incident X-ray source spectrum to an observed CCD PHA spectrum that takes into account the possibility of photon pileup. The success of the pileup model was demonstrated by its application to the moderately piled PHA spectrum of S5 0836 + 7104, observed by the *Chandra X-Ray Observatory* using the ACIS CCD detector. The model is sufficiently general that it should also be applicable to data obtained by the *XMM-Newton Observatory*.

In addition to being computationally efficient, the pileup equation makes use of standard X-ray spectral-analysis data products (ancillary response files and redistribution matrix files), and deals with the effects of grade migration through the spectral-fitting process. Hence, the model is ideally suited for incorporation into existing spectral-modeling software packages. It has already been added to the ISIS spectral-modeling program, which was used in this work for the analysis of the S5 0836 + 7104 CCD data.

I would like to thank Glenn Allen, Dan Dewey, David Huenemoerder, John Houck, and Herman Marshall for valuable discussions regarding the problem of pileup. I am also grateful to Dan Dewey and John Houck for their critical reading of the paper, and give special thanks to Claude Canizares for the use of the S5 0836 + 7104 dataset. Finally, I am deeply indebted to John Houck for making the necessary modifications to the ISIS spectral-modeling program to facilitate the testing of the pileup model. This work was supported under *Chandra X-Ray Center* contract SV 1-61010 from the Smithsonian Institution.

APPENDIX A

THE ISIS IMPLEMENTATION

This appendix describes the ISIS implementation of equation (32), which for a point source can be written

$$C_{\omega}(h) = N e^{-(\tau/\bar{\theta}_{\omega, \omega})} \int dE A_{\omega}(E) s(E) \int dE R(h, E) \sum_{p=1}^{\infty} \bar{G}_{p, \omega}(h) \frac{[\tau A_{\omega}(E) s(E)]^{*p}}{p!}. \quad (\text{A1})$$

As defined by equation (16), the effective area $A_{\omega}(E)$ includes the effects of the PSF. One can easily show (Davis 2001) that, as long as the mirror effective area does not vary much over the scale of the PSF, $A_{\omega}(E)$ can be factored as

$$A_{\omega}(E) = A(E) f_{\omega}(E), \quad (\text{A2})$$

where $f_{\omega}(E)$ represents the PSF fraction enclosed by the region ω .

Suppose that counts are extracted in some region Ω composed of multiple extraction cells. Then, the total number of counts $C_{\Omega}(h)$ with pulse height h expected in the region Ω is given by

$$C_{\Omega}(h) = \sum_{\omega \in \Omega} C_{\omega}(h), \quad (\text{A3})$$

where the sum extends over all detection cells contained in Ω .

The ISIS implementation makes several simplifying assumptions. The PSF fraction $f_{\omega}(E)$ is assumed to be independent of energy, although, strictly speaking, this assumption may not apply to very hard sources. In addition, the grade-migration functions are assumed to be given by the parameterization of equation (33).

One can always break the extraction region Ω into two subregions: one that suffers from pileup and one that does not. The pileup region can be further subdivided into n detection cells. For simplicity, the ISIS implementation assumes that each of these n detection cells has the same incident flux and contributes an equal expected number of counts. As a result, if f denotes the fraction of flux falling into the pileup region, then $1 - f$ is the fraction falling into the nonpileup region. It follows that the flux into each of the n detection cells is given by $fs(E)/n$.

The upshot of the above assumptions is that the pileup model implemented in ISIS can be written

$$C_{\Omega}(h) = (N\tau)(1 - f) \int dE R(h, E)A(E)s(E) + Nne^{-(\tau/\bar{g}_0) \int dE A(E) fs(E)/n} \sum_{p=1}^{\infty} \alpha^{p-1} \int dE R(h, E) \frac{[\tau A(E)fs(E)/n]^{*p}}{p!}, \quad (\text{A4})$$

where the first term represents the contribution from the nonpiled region and the second term represents the contribution from the n detection cells in the pileup region. Hence, the ISIS implementation contains four pileup-specific parameters: α , \bar{g}_0 , f , and n . For the analysis of the S5 0836 + 7104 data described in § 4, of these only α was allowed to vary, with the others fixed ($n = 1, f = 0.95, \bar{g}_0 = 1$).

It is worth mentioning that this particular implementation was coded for the analysis of *Chandra* data. As discussed in § 5, the analysis of *XMM-Newton* data may require the use of multiple detection cells, with a different PSF fraction in the central cell than in the surrounding cells. Hence, the ISIS implementation described above may not be directly applicable to the analysis of *XMM-Newton* data because it assumes the same PSF fraction in each cell. This implementation can still be applied to *XMM-Newton* data, but it may be necessary to analyze the counts in each detection cell separately.

REFERENCES

- Aschenbach, B., Briel, U., Haberl, F., Bräuninger, H., Burkert, W., Oppitz, A., Gondoin, P., & Lumb, D. 2000, Proc. SPIE, 4012, 731
- Ballet, J. 1999, A&AS, 135, 371
- Davis, J. E. 2001, ApJ, 548, 1010
- Fang, T., Marshall, H. L., Bryan, G. L., & Canizares, C. R. 2001, ApJ, 555, 356
- Gorenstein, P., Gursky, H., & Garmire, G. 1968, ApJ, 153, 885
- Houck, J. C., & DeNicola, L. A. 2000, in ASP Conf. Ser. 216, Astronomical Data Analysis Software and Systems IX, ed. N. Manset, C. Veillet, & D. Crabtree (San Francisco: ASP), 591
- Jerius, D., Donnelly, R. H., Tibbetts, R. J., Edgar, R. J., Gaetz, T. J., Schwartz, D. A., Speybroeck, L. P., & Zhao, P. 2000, Proc. SPIE, 4012, 17